

A Study of Six Extreme Low Mass Ratio Contact Binary Systems

SURJIT S. WADHWA,¹ BOJAN ARBUTINA,² JELENA PETROVIĆ,³ MIROSLAV D. FILIPOVIĆ,¹ AIN Y. DE HORTA,¹
NICK F. H. TOTHILL,¹ AND GOJKO DJURAŠEVIĆ³

¹*School of Science, Western Sydney University,
Locked Bag 1797, Penrith, NSW 2751, Australia.*

²*Department of Astronomy, Faculty of Mathematics, University of Belgrade, Studentski trg 16, 11000 Belgrade, Serbia.*

³*Astronomical Observatory, Volgina 7, 11060 Belgrade, Serbia*

ABSTRACT

Multi-band (B, V and R) photometric and spectroscopic observations of six poorly studied contact binaries carried out at the Western Sydney University and Las Cumbres Observatory were analysed using a recent version of the Wilson-Devenney code. All six were found to be of extreme low mass ratio ranging from 0.073 to 0.149. All are of F spectral class with the mass of the primary component ranging from $1.05M_{\odot}$ to $1.48M_{\odot}$. None show light curve features of enhanced chromospheric activity (O'Connell Effect) however five of the six do have significant ultraviolet excess indicating presence of increased magnetic and chromospheric activity. Period analysis based on available survey data suggests two systems have a slowly increasing period suggesting mass transfer from the secondary to the primary, two have a slow declining period with likely mass transfer from primary to the secondary while one shows a steady period and one undergoing transition from a declining to increasing period suggesting possible mass transfer reversal. We also compare light curve solutions against theoretical markers of orbital stability and show that three of six systems have mass ratios within the theoretical instability limit and maybe regarded as potential merger candidates.

Keywords: Red Nova, Contact Binary Merger, Low Mass Ratio

1. INTRODUCTION

Investigation of extreme low mass ratio contact binaries has recently seen heightened interest with view to identifying potential merger (red nova) progenitors (Wadhwa et al. 2021; Gazeas et al. 2021; Christopoulou et al. 2022; Liu et al. 2023). It has been known for some time that merger events and orbital instability in contact binaries is most likely when the mass ratio of the components ($q = M_2/M_1$) is below some critical value (Rasio & Shapiro 1995; Arbutina 2007, 2009). We have recently introduced methods to aid in the rapid identification of potential low mass ratio contact binary systems from survey photometry data (Wadhwa et al. 2022b) in addition to a theoretical framework linking the mass of the primary component and geometric elements determined through light curve analysis to orbital instability (Wadhwa et al. 2021).

We have previously reported analysis of fifteen extreme low mass ratio contact binaries with features of orbital instability (Wadhwa et al. 2022a, 2023). This study reports photometric and spectroscopic observations of six extreme low mass ratio poorly studied contact binary systems selected from the All Sky Automated Survey for SuperNovae (ASAS-SN) (Shappee et al. 2014; Jayasinghe et al. 2020). The systems were selected for observations based on the techniques described in Wadhwa et al. (2022b) as being likely of low mass ratio and potentially unstable. Identification details for the systems are summarised in Table 1. In addition to light curve analysis we show that at least 5 systems exhibit features of chromospheric activity without photospheric evidence for star spots.

2. PHOTOMETRIC AND SPECTROSCOPIC OBSERVATIONS

A1044 was observed over 5 nights in April 2020 with the Western Sydney University (WSU) 0.6m telescope equipped with a cooled SBIG 8300 CCD camera and standard Johnson *BVR* filters. All other systems were imaged using the 0.4m telescopes from the Las Cumbres Observatory (LCO) network. The LCO network telescopes acquire images using the SBIG STL-6303 CCD camera and Bessel *V, B* and Sloan *r'* filters. Images were acquired in *V* and *R/r'*

Table 1. Identifications, abbreviations, check and comparison stars for 6 studied systems

Name	Abbreviation	Comparison Star	Check Star
ASAS J054049-5527.8	A0540	2MASS 05403192-5527279	2MASS 05405378-5526306
ASAS J084220-0303.4	A0842	TYC 4867-806-11	TYC 4867-463-1
ASAS J103737-3709.5	A1037	TYC 7197-1470-1	TYC 7197-1596-1
ASAS J104422-0711.2	A1044	TYC 4919-253-1	2MASS 10441404-0710597
V565 Dra	V565 Dra	TYC 3897-742-1	2MASS 17383576+5710441
ASAS J200304-0256.0	A2003	TYC 5164-275-1	2MASS 10032574-0257207

bands for all systems except A0842 which was only observed in V band due to technical difficulties. To document the $B - V$ magnitude we also acquired between 40 and 50 images during eclipses in the B band. All images of A1044 were calibrated using multiple dark, flat and bias frames. The LCO network has an automated pipeline which provided calibrated images for all other systems. Differential photometry for each system was performed with the AstroImageJ (Collins et al. 2017) package using the comparison and check stars noted in Table 1. The comparison star magnitudes were adopted from the American Association of Variable Star Observers (AAVSO) Photometric All-Sky Survey (Henden et al. 2015). The AstroImageJ package estimates photometric errors and we excluded all observations where the estimated error was greater than 0.01 magnitude. Details of observations such as dates, observation numbers, exposure times along with light curve characteristics such as amplitude, maximum brightness, and $B - V$ colour are collated in Table 2.

Table 2. Details of observations, spectral class and light curve parameters. $(B - V)_o$ is distance and extinction corrected estimate.

Name	Date of Obs	Obs . (V, R)	Exp. Times (V, R)	Max Bright. (V)	Ampl. (V)	$B - V$	$(B - V)_o$	Sp. Type
A0540	11/22 - 01/23	310, 340	45s,40s	12.52	0.35	0.62	0.58	F9
A0842	02/23 - 02/23	375, -	45s,-	11.51	0.30	0.51	0.50	F8
A1037	02/23 - 05/23	420, 360	40s,35s	10.79	0.34	0.58	0.55	F9
A1044	04/20 - 05/20	415, 395	40s,33s	11.72	0.23	0.15	0.12	F0*
V565 Dra	06/22 - 05/23	460, 345	45s,40s	11.26	0.32	0.63	0.60	F7*
A2003	08/22 - 08/22	480, 550	40s,35s	10.51	0.41	0.68	0.53	F7

*Spectral classification from LAMOST survey.

Assessment of period variation, especially when small, requires high cadence long term (over many decades) observations. Given the lack of suitable historical observations no meaningful Observed-Computed ($O - C$) analysis could be performed for any of the systems. Instead we use the technique of employing periodic orthogonal polynomials and an analysis of variance statistic (a quality of fit marker) to fit multiple overlapping subsets, each of approximately 100 - 150 observations, of V or g' band survey photometry data for each system to estimate any significant period variations. The methodology is described in detail by Schwarzenberg-Czerny (1996) and was used by Tylenda et al. (2011) to demonstrate the exponential decay in the period of the only confirmed contact binary merger system V1309 Sco. We find that two of our systems (A540 and A2003) have a linear trend towards a reducing period, two systems (A0842 and A1037) have a linear trend of a rising period, V565 Dra has a shallow parabolic trend indicating a shift from falling to rising period while A1044 appears to have a relatively steady period. If one considers the transfer of mass as the only contributor to period change a rising period suggests mass transfer from the secondary to the primary and visa versa for a falling period. The period trends are summarised in Table 3 and illustrated in Figure 1.

Successful light curve analysis of contact binary systems without radial velocity data is only possible if complete eclipses are present (Terrell & Wilson 2005). During such analysis the temperature of the primary (T_1) is usually fixed as the shape of contact binary light curves is dependent almost exclusively on the geometric parameters such as the mass ratio, inclination and degree of contact. The light curve shape places a constrain on the component temperature ratio (T_2/T_1) but not on the absolute value of the component temperatures (Rucinski 1993, 2001). Notwithstanding the above, varied methods are used in assigning the temperature of the primary (T_1) with colour based estimations

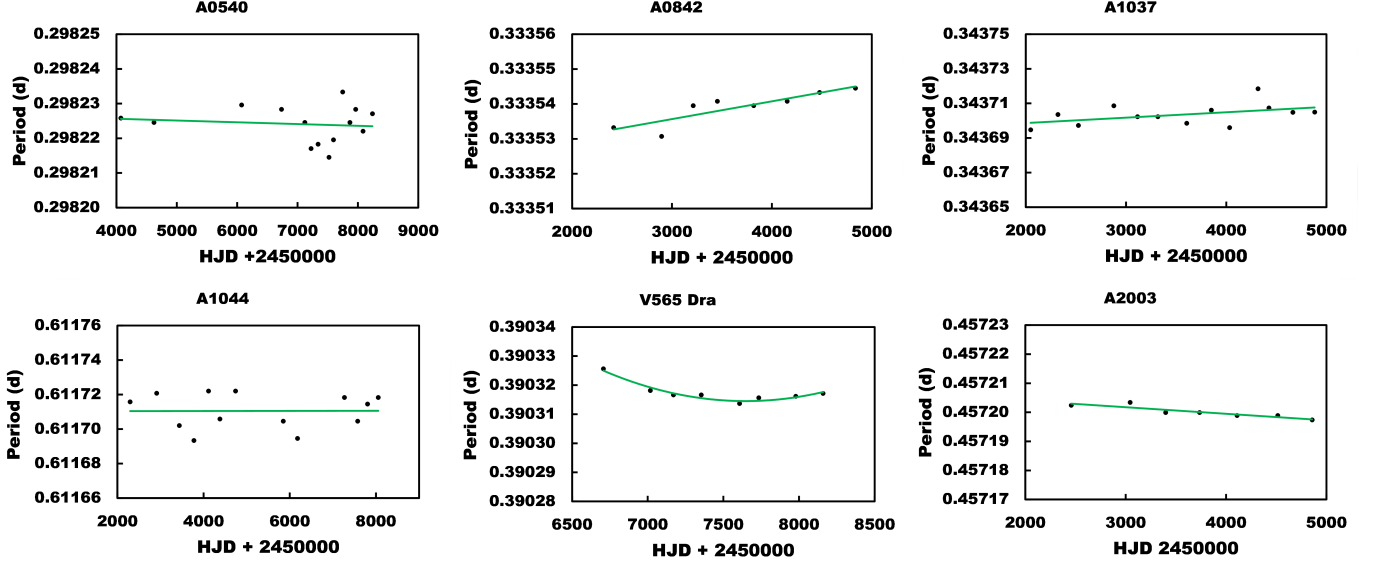


Figure 1. Period trend based on survey photometry data. The green line represents the best fit.

Table 3. Updated orbital elements and period trend.

Name	Epoch (HJD)	Period (d)	Period Trend (d/yr)
A0540	2459948.146810 ± 0.000250	0.2982187 ± 0.0000050	-1.87×10^{-7}
A0842	2459984.366616 ± 0.000309	0.3335395 ± 0.0000025	1.86×10^{-6}
A1037	2459986.138027 ± 0.000212	0.3434028 ± 0.0000015	1.15×10^{-6}
A1044	2458944.604343 ± 0.000052	0.6117118 ± 0.0000010	Steady
V565 Dra	2459752.674348 ± 0.000322	0.3903187 ± 0.0000025	Parabolic
A2003	2459811.109575 ± 0.000230	0.4571959 ± 0.0000030	-8.27×10^{-7}

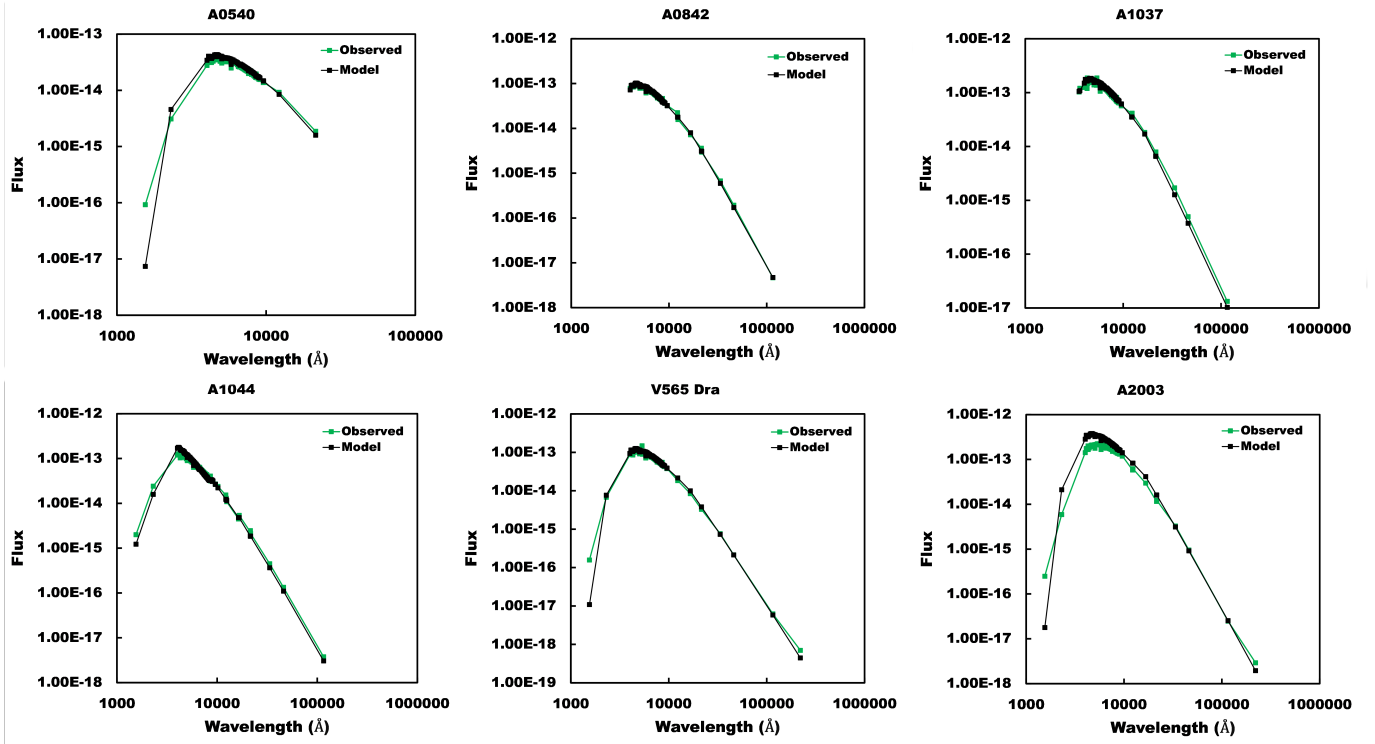
being employed most often. Colour calibrated estimates, although widely used, have been shown to be cumbersome. Recently in an analysis of four contact binaries Hu et al. (2022) found temperature variations between $B - V$ and $J - K$ colour calibrations in excess of 500K for 2 stars and 250K and 150K for the other two. Ma et al. (2023) reported variation in excess of 400K between spectra and space based survey colour databases. The VizieR database records a range in excess of 1000K for four of the systems reported here and many hundreds for the other two. Spectral classification of stars possibly represents an accurate and standard method and more recently many investigators (see e.g. Li et al. 2023; Guo et al. 2023; Chang et al. 2022; Guo et al. 2022) have adopted low resolution spectral class calibrations (where available) as an alternative to assign the usually fixed value for T_1 .

One mechanism to overcome the wide variations that can result from various templates and colour calibrations is through the investigation of the Spectral Energy Distribution (SED) constructed using photometric data from various bands collectively. Robitaille et al. (2007) and Bayo et al. (2008) performed comparison of the SEDs constructed from survey photometry with synthetic theoretical spectra and the modelled value for the effective temperature compared favourably to the theoretical spectral value. We compared the effective temperature of the systems (and hence temperature of the primary) determined through SED calibration against those estimated through spectral class for each system. Firstly, using the methodology described in Bayo et al. (2008) we constructed a photometry data set (SED) in different bands for each system from publicly available survey data. The constructed SEDs were then fitted to theoretical models which incorporated Kurucz atmospheres using χ^2 minimisation as described in Bayo et al. (2008) to determine the effective temperature. The SEDs and fitted model are illustrated in Figure 2. Two (A1044 and V565 Dra) of our six systems were observed with the The Large Sky Area Multi-Object Fiber Spectroscopic Telescope (LAMOST) (Luo et al. 2018) with the reported spectral classes F0 and F7, respectively. For the other four systems we used the 2m telescopes from the LCO network equipped with the low resolution FLOYDS spectrograph to acquire spectra that were compared to standard main sequence star spectra from Jacoby et al. (1984); Pickles (1998) to de-

Table 4. Effective temperature (K) range as reported in the VizieR database, SED modelling and spectral class interpolation.

Name	VizieR Range	SED	Spec. Class
A0540	5818 - 6874	6000	6050
A0842	5959 - 6740	6250	6180
A1037	5305 - 6338	6000	6050
A1044	6632 - 7793	7250	7200
V565 Dra	5921 - 7044	6250	6280
A2003	5006 - 5773	5750	6280

termine the spectral class for each system as recorded in Table 2. Selected FLOYDS spectra and matched library spectra are shown in Figure 3. We used the April 2022 update of Pecaut & Mamajek (2013) calibration tables of spectral class and temperature for main sequence stars to determine the spectral based temperature of the primary component. The VizieR range, SED and spectral class effective temperatures are summarised in Table 4. From Table 4 we see that in all cases except A2003, where the variation between SED and spectral effective temperature varies by more than 500K, there is good agreement between a collective photometric approach and spectral class for estimating the effective temperature. The findings are very similar to Panchal et al. (2022) who also found close agreement between spectral class effective temperature and SED modelled values. The difference in A2003 most likely, although not for certain, relates to the relative high extinction for the system with an estimated distance corrected extinction of 0.48 magnitudes. Overall we consider that the recent trend towards the use of low resolution spectra and spectral classification to assign a fixed value to the temperature of the primary to be valid and we have used this method for light curve analysis of the systems presented in this study.

**Figure 2.** Observed and modelled SEDs for all six systems. The observed photometry is indicated in green and the fitted model in black. The flux on the vertical axes is in $\text{erg}/\text{cm}^2/\text{s}/\text{\AA}$. The wavelength is in Angstroms (\AA). Both axes are in log scale.

3. LIGHT CURVE ANALYSIS

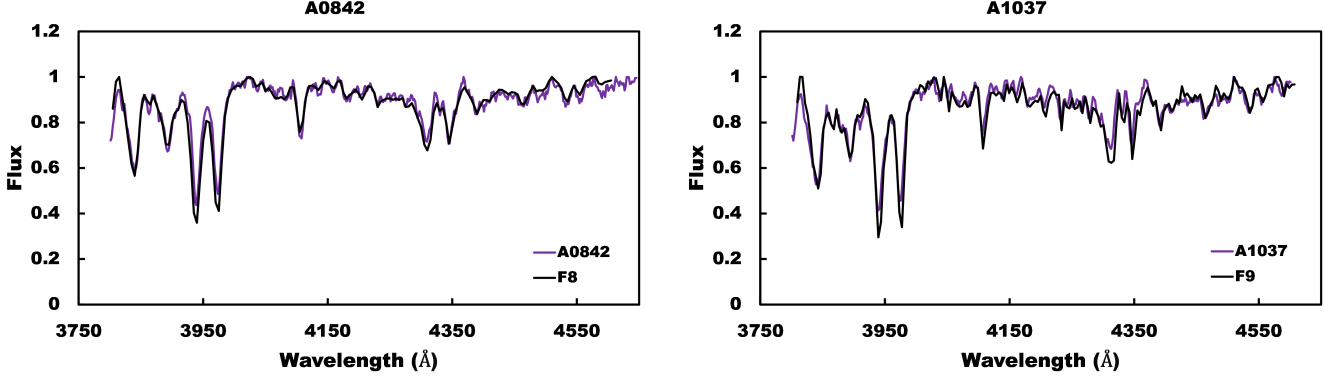


Figure 3. Observed (low resolution) and matched library spectra for A0842 and A1037.

We confirm that all systems show total eclipses and as such determination of the mass ratio from photometry alone would be possible. As there is no significant asymmetry in the maximum brightness only unspotted solutions were modelled. We used the Wilson-Devinney (WD) code (2013 version) which incorporates Kurucz atmospheres to model simultaneous V and R band light curve solutions (Nelson 2021; Kallrath et al. 1998; Wilson 1990). Since the effective temperature of the primary is below 7500K for each system, the gravity darkening coefficients were set equal $g_1 = g_2 = 0.32$, and bolometric albedoes as $A_1 = A_2 = 0.5$. we used the logarithmic limb darkening coefficients from van Hamme (1993) as advocated by Nelson & Robb (2015).

We searched for the mass ratio (q) for the systems using the grid method first described by (Russo & Sollazzo 1982). Systematic search was made for a range of fixed values for the mass ratios from 0.05 to 15. A coarse search was performed up to $q = 1$ in increments of 0.1 and in increments of 0.2 up to $q = 15$. The search was then refined in increments of 0.01 near the best solution. During the search procedure the temperature of the secondary component (T_2), the surface potential (Ω) (i.e. fillout f), orbital inclination (i) and the dimensionless luminosity of the primary (L_1) were all treated as adjustable parameters. For each mass ratio, iterations were executed until the reported standard deviations were higher than the suggested adjustment for all parameters. To obtain the full solution the mass ratio was also made an adjustable parameter during the last iteration and the suggested standard deviations for each parameter was recorded as the potential error. Summary of the light curve solutions is presented in Table 5. Observed and WD fitted light curves are illustrated in Figure 4.

4. ABSOLUTE PARAMETERS AND ORBITAL STABILITY

4.1. Absolute Parameters

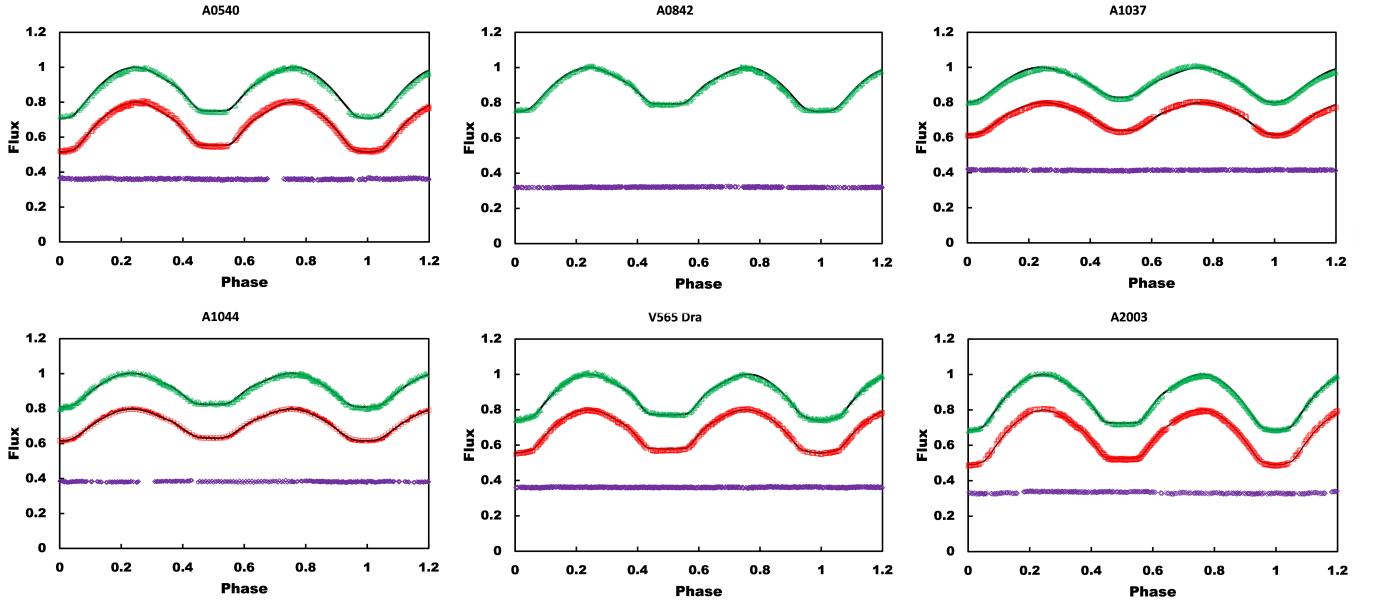
Full investigation of astrophysical phenomenon such as orbital stability and chromospheric activity requires knowledge of the absolute physical parameters especially the mass of the primary. Without high resolution spectroscopic observations one is reliant on indirect methods to estimate the mass of the primary component. In this study we use the mean of a distance based estimate and a colour calibration based estimate of the mass of the primary. It is accepted that the primary component of contact binaries follow zero age main sequence profile (Yildiz & Doğan 2013). For our colour based estimation we used the 2MASS $J - H$ magnitudes (Skrutskie et al. 2006) for each system and the calibration tables of Pecaut & Mamajek (2013) (April 2022 update) for low mass ($0.6M_\odot < M_1 < 1.6M_\odot$) stars to interpolate the mass of the primary component.

The distance based estimation was interpolated from the absolute magnitude of the primary component corrected for extinction. The absolute magnitude of the primary component was determined as follows: As all systems have total eclipses and are of low mass ratio the secondary eclipse apparent magnitude represents the apparent magnitude of the primary. We obtained the absolute magnitude of the primary (M_{V1}) using the GAIA EDR 3 (Anders et al. 2022) distance and the line of sight extinction corrected for distance ($E(B - V)_d$) as described in Wadhwa et al. (2023). The absolute magnitude was obtained using the standard distance module. The observed $B - V$ was also corrected for extinction ($B - V)_o$ as:

$$(B - V)_o = (B - V) - E(B - V)_d. \quad (1)$$

Table 5. Light curve solution and other absolute parameters for six investigated contact binary systems.

	A0540	A0842	A1037	A1044	V565 Dra	A2003
T_1 (K) (Fixed)	6050	6180	6050	7200	6280	6280
T_2 (K)	5884 ± 16	5997 ± 27	5741 ± 34	7190 ± 27	6259 ± 11	6266 ± 10
Incl. ($^\circ$)	82.3 ± 0.9	77.5 ± 1.4	68.1 ± 0.8	72.7 ± 0.5	$90.0^{+0.0}_{-0.5}$	82.5 ± 0.5
q	0.14 ± 0.001	0.100 ± 0.006	0.090 ± 0.003	0.073 ± 0.003	0.108 ± 0.002	0.149 ± 0.002
q_{inst} ($f=0$)	0.083 ± 0.006	0.084 ± 0.003	0.074 ± 0.003	0.048 ± 0.001	0.080 ± 0.013	0.093 ± 0.005
q_{inst} ($f=1$)	0.094 ± 0.008	0.096 ± 0.004	0.086 ± 0.004	0.053 ± 0.001	0.091 ± 0.017	0.108 ± 0.006
Fillout (%)	69 ± 2	83 ± 4	57 ± 4	83 ± 3	71 ± 2	82 ± 2
r_1 (mean)	0.578	0.605	0.604	0.625	0.596	0.578
r_2 (mean)	0.259	0.239	0.219	0.216	0.238	0.271
M_1/M_\odot	1.13 ± 0.05	1.12 ± 0.03	1.18 ± 0.02	1.48 ± 0.05	1.15 ± 0.11	1.05 ± 0.03
M_2/M_\odot	0.16 ± 0.02	0.11 ± 0.02	0.11 ± 0.01	0.11 ± 0.01	0.12 ± 0.03	0.16 ± 0.02
M_{V1}	3.76 ± 0.20	4.16 ± 0.10	3.97 ± 0.10	2.43 ± 0.21	3.77 ± 0.48	4.41 ± 0.15
A/R_\odot	2.04 ± 0.02	2.17 ± 0.01	2.25 ± 0.02	3.53 ± 0.03	2.44 ± 0.09	2.65 ± 0.01
R_1/R_\odot	1.18 ± 0.02	1.31 ± 0.01	1.36 ± 0.02	2.21 ± 0.03	1.45 ± 0.05	1.53 ± 0.01
R_2/R_\odot	0.53 ± 0.02	0.52 ± 0.01	0.49 ± 0.02	0.76 ± 0.02	0.58 ± 0.03	0.72 ± 0.01
$\Delta\rho$	-0.54	-0.43	-0.60	-0.15	-0.37	-0.18
UV Excess	-1.75	-1.53	–	-4.17	-2.28	-1.43

**Figure 4.** The WD model (black line) and observed V band (open green triangle), R band (open red square) light curves for the six reported systems. The open purple diamonds represents the check star. The flux has been arbitrarily shifted vertically for clarity

The extinction corrected $(B - V)_o$ values are summarised in Table 2 while the estimated absolute magnitudes are summarised in Table 5 along with other absolute parameters.

The distance based mass of the primary was obtained from interpolation of the absolute magnitude and mass of main sequence stars from the calibration tables of Pecaut & Mamajek (2013) (April 2022 update) for low mass ($0.6M_\odot < M_1 < 1.6M_\odot$) stars. The distance based estimate resulted in the largest error and this was adopted as the error for the mass estimation. All other errors were propagated from this estimation. The mass of the secondary (M_2) was determined from the mass ratio and Kepler's third law used to derive the current separation (A) between

the components. The light curve solution provides an estimate of the fractional radii of the components ($r_{1,2}$) for three orientations. The geometric mean of these was used to estimate the absolute radii ($R_{1,2}$) of the components by applying $R_1 = r_1 A$ and $R_2 = r_2 A$ as per [Awadalla & Hanna \(2005\)](#). All the absolute parameters are summarised in [Table 5](#).

It been well established that the secondary components have larger radii than main sequence stars of similar mass. [Wadhwa et al. \(2022b\)](#) also reported that the radius of the primary may also be more than 25% larger than corresponding main sequence stars. In addition to change in the radii of the components some researchers ([Yildiz & Doğan 2013](#)) suggest that evolutionary mechanisms will likely lead to significant density variation between the components such that the secondary will always be denser and the the difference between density of the primary and secondary components ($\Delta\rho$) will always be less than zero ([Kähler 2004](#)).

As noted above the light curve solution provides fractional radii for each component and one can use geometric mean of these along with Equation (3) from ([Mochnicki 1981](#)) to calculate the density difference ($\Delta\rho$). All our system show that the density of the secondary is indeed higher and that $\Delta\rho$ is negative. The results are summarised in [Table 5](#).

4.2. Orbital Stability

The merger potential of contact binary systems and their orbital stability has received significant attention recently ([Wadhwa et al. 2021](#); [Liu et al. 2023](#); [Christopoulou et al. 2022](#)). New mathematical relations linking the instability mass ratio, mass of the primary and the degree of contact have recently been reported by [Wadhwa et al. \(2021\)](#) who showed that for low mass primaries ($0.6M_\odot < M_1 < 1.6M_\odot$) the instability mass ratio (q_{inst}) is between:

$$q_{inst} = 0.1269M_1^2 - 0.4496M_1 + 0.4403 \quad (f = 1) \quad (2)$$

and

$$q_{inst} = 0.0772M_1^2 - 0.3003M_1 + 0.3237 \quad (f = 0). \quad (3)$$

The above equations represent the extremes of the instability mass ratio at marginal contact ($f = 0$) and full over-contact ($f = 1$).

We calculate the instability mass ratio range (q_{inst}) for each system and provide it [Table 5](#). Although all six systems have extreme low mass ratios only three (A0842, A1037 and V565 Dra) can be classified as being potential merger candidates with modelled mass ratios within the error range for the instability mass ratio. A0540, A1044 and A2003 all have modelled mass ratios well above the instability mass ratio range and as such must be considered likely stable. As all systems described are relatively bright and well within the reach of modest instruments regular monitoring of the potential merger candidates even by advanced amateurs should be encouraged.

5. HIGH ENERGY INDICATORS OF CHROMOSPHERIC ACTIVITY

Contact binary systems usually have periods of less than 24 hours with synchronised rotation. Magnetic activity is thought to be high in rapidly rotating systems including contact binaries ([Gharami et al. 2019](#)) resulting in increased stellar magnetic wind and magnetic breaking. Increased magnetic breaking will eventually lead to loss of angular momentum from the system and potential orbital instability ([Li et al. 2004](#)). The only significant photospheric indicator of increased magnetic activity is the presence of star spots usually manifesting as the O'Connell effect or asymmetric maxima of the light curve. The photosphere is dominated by high intensity low energy emissions which obscure lesser intensive chromospheric emissions therefore light curve analysis provides little indication of chromospheric activity. Direct measure of angular momentum loss is difficult, nevertheless, secondary indicators of enhanced magnetic and chromospheric activity ([Vilhu 1983](#); [Rucinski & Vilhu 1983](#); [Li et al. 2004](#)) are potentially easier to observe. The six systems described in this report do not demonstrate photometric features of enhanced magnetic/chromospheric activity. Significant chromospheric and magnetic activity however is not excluded. Emissions at higher energy levels such as the far ultraviolet band can provide a clearer indicator of such activity. The GALEX (Galaxy Evolution Explorer) satellite surveyed the sky in both the far-ultraviolet band (FUV) centered on 1539 Å and near-ultraviolet band (NUV) centered on 2316 Å. Only the FUV band can be relied upon for the detection of chromospheric activity as NUV emissions may also be contaminated by photospheric emissions ([Smith & Redenbaugh 2010](#)).

As demonstrated by ([Noyes et al. 1984](#); [Henry et al. 1996](#)) the R'_{HK} index and $\log R'_{HK} \geq -4.75$ are characteristic indicators of a more active star. [Smith & Redenbaugh \(2010\)](#) matched GALEX FUV magnitudes (m_{FUV}) to the

$\log R'_{\text{HK}}$ for dwarf stars to derive the $\Delta(m_{\text{FUV-B}})$ colour excess:

$$\Delta(m_{\text{FUV-B}}) = (m_{\text{FUV}} - B) - (m_{\text{FUV}} - B)_{\text{base}} \quad (4)$$

where

$$(m_{\text{FUV}} - B)_{\text{base}} = 6.73(B - V) + 7.43, \quad (5)$$

They concluded that chromospherically active stars have a UV colour excess below -0.5 while those with lesser chromospheric and magnetic activity have a colour excess above -0.5.

The GALEX mission observed five of our six systems with measured FUV magnitudes. Ultraviolet colour excess was calculated for all five using Equations 4 & 5. All five have ultraviolet colour excess well below -0.5, a value suggestive of enhanced magnetic/chromospheric activity in the absence of photospheric features. It is well known that magnetically active features such as plages (Hall 2008) may be associated with star spots, however, the reverse is not always the case – chromospheric/magnetic activity without photospheric features is possible (Mandal et al. 2017). Table 5 summarises the the UV colour excesses for the five systems observed by GALEX

6. SUMMARY AND CONCLUSION

The confirmation that the red nova V1309 Sco in 2008 was indeed a merger event between components of a contact binary system (Tylenda et al. 2011) has significantly increased interest in the study of contact binaries. Although it has been known for some time that merger events are likely at low mass ratios (Rasio & Shapiro 1995; Arbutina 2007, 2009) most investigators until more recently have sought to define a minimum mass ratio at which orbital stability is likely. Recent theoretical updates (Wadhwa et al. 2021) would indicate that the global minimum mass ratio is of little practical use and instead orbital instability onset is dependent on the mass of the primary component and that for low mass systems instability can occur with mass ratios as high as 0.22 to below 0.05.

The number of identified contact binaries is ever increasing with new systems being continually added through various sky surveys. Large scale high resolution radial velocity observations are at present impractical thus limiting our search for potential merger candidates among systems demonstrating total eclipses and therefore suitable for light curve analysis. To this end Wadhwa et al. (2022b) have introduced simplified techniques to identify potential extreme low mass ratio system from survey photometric data. The present study continues our programme of follow-up dedicated observations of potential merger candidates identified from such data. We report photometry and spectroscopic observations of six contact binaries identified as potential extreme low mass ratio systems from the ASAS-SN survey. All six are confirmed as being of extreme low mass ratio, having a mass ratio less than 0.15. Three systems fall into the instability category based on theoretical considerations. It must be noted that the instability mass ratio is highly dependent on the mass of the primary and a 10% change in the primary’s mass can result in up to a 17% change in the instability mass ratio (Christopoulou et al. 2022) so confirmation of the mass of the primary, in particular for three potentially unstable systems (A0842, A1037 and V565 Dra) through high resolution spectral observations would be desirable.

Compared to other contact binaries the six systems reported here follow similar characteristics with significantly larger and brighter secondaries relative to main sequence counterparts. In addition, the secondary component in all cases is significantly denser than the primary component. Extreme low mass ratio contact binaries usually show photospheric signs of increased magnetic and chromospheric activity as a variation in the two maxima in the light curve due to the presence of star spots. The current sample of six did not show significant variation in maxima, however, non-photospheric markers such as increased high energy emissions, particularly in the far ultraviolet band, were present in all five of the systems observed by the GALEX mission.

Recent progress in the rapid identification of low mass ratio systems from survey photometry and theoretical considerations for orbital stability has significantly increased the detection of potentially unstable system. As noted above, we have already reported 15 such systems and the current study adds a further three. The study also highlights that not all extreme low mass ratio systems will be unstable, three systems from the current study and some previous large surveys with over 10 systems in each study did not detect any unstable system even though they all reported extreme low mass ratio systems (Liu et al. 2023; Gazeas et al. 2021; Christopoulou et al. 2022; Li et al. 2022).

Acknowledgements.

Based on data acquired on the Western Sydney University, Penrith Observatory Telescope. We acknowledge the traditional custodians of the land on which the Observatory stands, the Dharug people, and pay our respects to elders past and present.

This research has made use of the SIMBAD database, operated at CDS, Strasbourg, France.

This work makes use of observations from the Las Cumbres Observatory global telescope network.

This publication makes use of VOSA, developed under the Spanish Virtual Observatory (<https://svo.cab.inta-csic.es>) project funded by MCIN/AEI/10.13039/501100011033/ through grant PID2020-112949GB-I00. VOSA has been partially updated by using funding from the European Union’s Horizon 2020 Research and Innovation Programme, under Grant Agreement number 776403 (EXOPLANETS-A).

B. Arbutina acknowledges the funding provided by the Ministry of Science, Technological Development and Innovation of the Republic of Serbia through the contract 451-03-47/2023-01/200104.

During work on this paper, G. Djurašević and J. Petrović were financially supported by the Ministry of Science, Technological Development and Innovation of the Republic of Serbia through contract 451-03-47/2023-01/200002

REFERENCES

- Anders, F., Khalatyan, A., Queiroz, A. B. A., et al. 2022, *A&A*, 658, A91, doi: [10.1051/0004-6361/202142369](https://doi.org/10.1051/0004-6361/202142369)
- Arbutina, B. 2007, *MNRAS*, 377, 1635, doi: [10.1111/j.1365-2966.2007.11723.x](https://doi.org/10.1111/j.1365-2966.2007.11723.x)
- . 2009, *MNRAS*, 394, 501, doi: [10.1111/j.1365-2966.2008.14332.x](https://doi.org/10.1111/j.1365-2966.2008.14332.x)
- Awadalla, N. S., & Hanna, M. A. 2005, *Journal of Korean Astronomical Society*, 38, 43, doi: [10.5303/JKAS.2005.38.2.043](https://doi.org/10.5303/JKAS.2005.38.2.043)
- Bayo, A., Rodrigo, C., Barrado Y Navascués, D., et al. 2008, *A&A*, 492, 277, doi: [10.1051/0004-6361:200810395](https://doi.org/10.1051/0004-6361:200810395)
- Chang, L.-F., Zhu, L.-Y., Sarotsakulchai, T., & Soonthornthum, B. 2022, *PASJ*, 74, 1421, doi: [10.1093/pasj/psac080](https://doi.org/10.1093/pasj/psac080)
- Christopoulou, P.-E., Lalounta, E., Papageorgiou, A., et al. 2022, *MNRAS*, 512, 1244, doi: [10.1093/mnras/stac534](https://doi.org/10.1093/mnras/stac534)
- Collins, K. A., Kielkopf, J. F., Stassun, K. G., & Hessman, F. V. 2017, *AJ*, 153, 77, doi: [10.3847/1538-3881/153/2/77](https://doi.org/10.3847/1538-3881/153/2/77)
- Gazeas, K. D., Loukaidou, G. A., Niarchos, P. G., et al. 2021, *MNRAS*, 502, 2879, doi: [10.1093/mnras/stab234](https://doi.org/10.1093/mnras/stab234)
- Gharami, P., Ghosh, K., & Rahaman, F. 2019, *Bulgarian Astronomical Journal*, 31, 97
- Guo, D., Li, K., Liu, F., et al. 2023, *PASP*, 135, 044201, doi: [10.1088/1538-3873/accc55](https://doi.org/10.1088/1538-3873/accc55)
- Guo, D.-F., Li, K., Liu, F., et al. 2022, *MNRAS*, 517, 1928, doi: [10.1093/mnras/stac2811](https://doi.org/10.1093/mnras/stac2811)
- Hall, J. C. 2008, *Living Reviews in Solar Physics*, 5, 2, doi: [10.12942/lrsp-2008-2](https://doi.org/10.12942/lrsp-2008-2)
- Henden, A. A., Levine, S., Terrell, D., & Welch, D. L. 2015, in *American Astronomical Society Meeting Abstracts*, Vol. 225, American Astronomical Society Meeting Abstracts #225, 336.16
- Henry, T. J., Soderblom, D. R., Donahue, R. A., & Baliunas, S. L. 1996, *AJ*, 111, 439, doi: [10.1086/117796](https://doi.org/10.1086/117796)
- Hu, K., Meng, Z.-B., Wang, H.-W., Yu, Y.-X., & Xiang, F.-Y. 2022, *PASA*, 39, e057, doi: [10.1017/pasa.2022.53](https://doi.org/10.1017/pasa.2022.53)
- Jacoby, G. H., Hunter, D. A., & Christian, C. A. 1984, *ApJS*, 56, 257, doi: [10.1086/190983](https://doi.org/10.1086/190983)
- Jayasinghe, T., Stanek, K. Z., Kochanek, C. S., et al. 2020, *MNRAS*, 491, 13, doi: [10.1093/mnras/stz2711](https://doi.org/10.1093/mnras/stz2711)
- Kähler, H. 2004, *A&A*, 414, 317, doi: [10.1051/0004-6361:20031629](https://doi.org/10.1051/0004-6361:20031629)
- Kallrath, J., Milone, E. F., Terrell, D., & Young, A. T. 1998, *ApJ*, 508, 308, doi: [10.1086/306375](https://doi.org/10.1086/306375)
- Li, K., Gao, X., Liu, X.-Y., et al. 2022, *AJ*, 164, 202, doi: [10.3847/1538-3881/ac8ff2](https://doi.org/10.3847/1538-3881/ac8ff2)
- Li, K.-X., Li, K., Liu, F., et al. 2023, *PASP*, 135, 054201, doi: [10.1088/1538-3873/acc7cb](https://doi.org/10.1088/1538-3873/acc7cb)
- Li, L., Han, Z., & Zhang, F. 2004, *MNRAS*, 355, 1383, doi: [10.1111/j.1365-2966.2004.08457.x](https://doi.org/10.1111/j.1365-2966.2004.08457.x)
- Liu, X.-Y., Li, K., Michel, R., et al. 2023, *MNRAS*, 519, 5760, doi: [10.1093/mnras/stad026](https://doi.org/10.1093/mnras/stad026)

- Luo, A. L., Zhao, Y. H., Zhao, G., & et al. 2018, *VizieR Online Data Catalog*, V/153
- Ma, S., Liu, J., Zhang, Y., et al. 2023, *Research in Astronomy and Astrophysics*, 23, 035012, doi: [10.1088/1674-4527/acb97f](https://doi.org/10.1088/1674-4527/acb97f)
- Mandal, S., Chatterjee, S., & Banerjee, D. 2017, *ApJ*, 835, 158, doi: [10.3847/1538-4357/835/2/158](https://doi.org/10.3847/1538-4357/835/2/158)
- Mochnacki, S. W. 1981, *ApJ*, 245, 650, doi: [10.1086/158841](https://doi.org/10.1086/158841)
- Nelson, R. H. 2021, *New Astron*, 86, 101565, doi: [10.1016/j.newast.2020.101565](https://doi.org/10.1016/j.newast.2020.101565)
- Nelson, R. H., & Robb, R. M. 2015, *Information Bulletin on Variable Stars*, 6134, 1
- Noyes, R. W., Hartmann, L. W., Baliunas, S. L., Duncan, D. K., & Vaughan, A. H. 1984, *ApJ*, 279, 763, doi: [10.1086/161945](https://doi.org/10.1086/161945)
- Panchal, A., Joshi, Y. C., De Cat, P., & Tiwari, S. N. 2022, *ApJ*, 927, 12, doi: [10.3847/1538-4357/ac45fb](https://doi.org/10.3847/1538-4357/ac45fb)
- Pecaut, M. J., & Mamajek, E. E. 2013, *ApJS*, 208, 9, doi: [10.1088/0067-0049/208/1/9](https://doi.org/10.1088/0067-0049/208/1/9)
- Pickles, A. J. 1998, *PASP*, 110, 863, doi: [10.1086/316197](https://doi.org/10.1086/316197)
- Rasio, F. A., & Shapiro, S. L. 1995, *ApJ*, 438, 887, doi: [10.1086/175130](https://doi.org/10.1086/175130)
- Robitaille, T. P., Whitney, B. A., Indebetouw, R., & Wood, K. 2007, *ApJS*, 169, 328, doi: [10.1086/512039](https://doi.org/10.1086/512039)
- Rucinski, S. M. 1993, *PASP*, 105, 1433, doi: [10.1086/133326](https://doi.org/10.1086/133326)
- . 2001, *AJ*, 122, 1007, doi: [10.1086/321153](https://doi.org/10.1086/321153)
- Rucinski, S. M., & Vilhu, O. 1983, *MNRAS*, 202, 1221, doi: [10.1093/mnras/202.4.1221](https://doi.org/10.1093/mnras/202.4.1221)
- Russo, G., & Sollazzo, C. 1982, *A&A*, 107, 197
- Schwarzenberg-Czerny, A. 1996, *ApJL*, 460, L107, doi: [10.1086/309985](https://doi.org/10.1086/309985)
- Shappee, B. J., Prieto, J. L., Grupe, D., et al. 2014, *ApJ*, 788, 48, doi: [10.1088/0004-637X/788/1/48](https://doi.org/10.1088/0004-637X/788/1/48)
- Skrutskie, M. F., Cutri, R. M., Stiening, R., et al. 2006, *AJ*, 131, 1163, doi: [10.1086/498708](https://doi.org/10.1086/498708)
- Smith, G. H., & Redenbaugh, A. K. 2010, *PASP*, 122, 1303, doi: [10.1086/657051](https://doi.org/10.1086/657051)
- Terrell, D., & Wilson, R. E. 2005, *Ap&SS*, 296, 221, doi: [10.1007/s10509-005-4449-4](https://doi.org/10.1007/s10509-005-4449-4)
- Tylenda, R., Hajduk, M., Kamiński, T., et al. 2011, *A&A*, 528, A114, doi: [10.1051/0004-6361/201016221](https://doi.org/10.1051/0004-6361/201016221)
- van Hamme, W. 1993, *AJ*, 106, 2096, doi: [10.1086/116788](https://doi.org/10.1086/116788)
- Vilhu, O. 1983, *Highlights of Astronomy*, 6, 643
- Wadhwa, S. S., Arbutina, B., Tothill, N. F. H., et al. 2023, *arXiv e-prints*, arXiv:2306.15190. <https://arxiv.org/abs/2306.15190>
- Wadhwa, S. S., De Horta, A., Filipović, M. D., et al. 2021, *MNRAS*, 501, 229, doi: [10.1093/mnras/staa3637](https://doi.org/10.1093/mnras/staa3637)
- . 2022a, *Research in Astronomy and Astrophysics*, 22, 105009, doi: [10.1088/1674-4527/ac8b59](https://doi.org/10.1088/1674-4527/ac8b59)
- Wadhwa, S. S., De Horta, A. Y., Filipović, M. D., et al. 2022b, *Journal of Astrophysics and Astronomy*, 43, 94, doi: [10.1007/s12036-022-09888-7](https://doi.org/10.1007/s12036-022-09888-7)
- Wilson, R. E. 1990, *ApJ*, 356, 613, doi: [10.1086/168867](https://doi.org/10.1086/168867)
- Yildiz, M., & Doğan, T. 2013, *MNRAS*, 430, 2029, doi: [10.1093/mnras/stt028](https://doi.org/10.1093/mnras/stt028)